Cardanol-Based Polyurethane Coatings via Click Chemistry: An Eco-friendly Approach

Kunal Wazarkar and Anagha Sabnis*

Department of Polymer and Surface Engineering, Institute of Chemical Technology, Nathalal Parekh Marg, Matunga (E), Mumbai - 400019, India

ABSTRACT: This research work discloses the preparation of polyurethane coatings from cardanol modified using thiol-ene chemistry, wherein unsaturated long alkyl chain of cardanol was successfully utilized via thiol-ene click reaction to synthesize polyol. For this purpose, cardanol and thioglycerol was reacted in the presence of Irgacure 184 (photoinitiator) and 1,8-Diazabicyclo[5.4.0]undec-7-ene (catalyst) and exposed to UV light for 12 h at 80 °C. One mole of thioglycerol was successfully added across the double bond of fatty chain of cardanol and confirmed by chemical and spectroscopic analysis. Further, the polyol thus prepared was cured with various polyisocyanates, viz., N-75 (HDI based), L-67/BA (TDI based), Z-4470 (IPDI based) and corresponding polyurethane coatings were developed. The coatings were then analyzed for mechanical, chemical, optical, thermal and anticorrosive properties. It was observed that cardanol-based PU coatings exhibited excellent mechanical, chemical and thermal and anticorrosive properties as compared to that of commercial acrylic-PU coatings.

KEYWORDS: Thiol-ene, click chemistry, polyurethane, anticorrosive, ultraviolet light

1 INTRODUCTION

Polyurethane (PU) is the sixth most used synthetic polymer in practically all fields of industrial applications such as foams, elastomers, thermoplastics, thermosets, adhesives, coatings, sealants, fibers and many more [1–4]. Usually PUs are made by addition polymerization of petroleum-based isocyanates with hydroxyl functional compound to generate the urethane linkages [5–7].

Recently, the shortage of petroleum-derived materials and their environmental effects have forced researchers to explore various biomaterials that are derived from renewable resources and are abundantly available in nature. For polymer and coating applications, most commonly, vegetable oils, cellulose, starch, sucrose, sugar, lignin, cashew nut shell liquid (CNSL), etc., and their derivatives have already been explored in the past. Amongst these, CNSL is a major raw material and contains phenolic compounds, viz., cardol, 2-methyl cardol, cardanol and anacardic acid [8, 9]. Due to its interesting functionalities and balanced

structure, cardanol is considered to be the most efficient and suitable candidate for a number of industrial applications like resins, paints and coatings, adhesives, lacquers and hybrid materials [10, 11]. Traditionally, polyurethanes were prepared by crosslinking isocyanates with oil-based polyol which was synthesized by epoxidation of double bonds followed by ring-opening reaction with nucleophiles [12]. However, the process of synthesizing polyol is tedious and time consuming.

In 2001, Sharpless *et al.* introduced the term "click reaction" for the reactions which are insensitive to oxygen and moisture, result in very high product yield, are simple to perform in short reaction time and form minor by-products and can be conducted in solvent-free or easily removable solvent media [13–16]. Thiol-ene addition is a type of "click reaction" wherein the weak sulphur hydrogen bond present in the thiol compounds can undergo various chemical reactions to produce a variety of useful monomers and oligomers for polymer and coating applications [17–20].

Various factors need to be considered while carrying out this reaction: a) The reactivity of alkenes varies significantly depending on the nature of C=C bond. For example, addition of thiols across terminal double bonds (eugenol, vinyl ethers, etc.) is much more efficient than that across the highly strained double bonds

(norborene, double bonds in vegetable oils, etc.). b) The reaction can be catalyzed by the addition of nucleophilic catalysts such as phosphines and amines, as it hinders the probability of polymerization of C=C-containing compounds [21].

Because of its high efficiency and simple operation [22], thiol-ene addition reaction has received a lot of attention recently. In polymer and coating industries, thiol-ene reaction is adopted to synthesize resins and polymers for numerous applications, including protective coatings and films, adhesives, optical displays, nano-imprinting, microfluidic devices, complex surface patterns, optical switching arrays, and high impact energy-absorbing devices. Various biobased materials have been utilized for thiol-ene reactions to obtain a variety of products. Yoshimura *et al.* developed polymer networks by adding various thiol compounds across allyl-etherified eugenol derivatives [22]. Some of the oils such as grapeseed oil [23, 24], linseed oil [25], soyabean oil [26–28], sunflower oil, and castor oils [29–30] were modified with thiol-ene reaction for various applications in the polymer industry [31]. Recently, cardanol-based polyols were synthesized via thiol-ene addition using mercaptoethanol and subsequently polyurethane coatings were prepared. It was concluded that the resultant coatings exhibited good mechanical and chemical properties [32].

The main objective of the present work is to study the effect of various isocyanate curing agents on the performance properties of polyurethane coatings prepared using thiol-ene coupling of cardanol. It is obvious that the varying structure of isocyanates will significantly change the performance properties. In addition, the sulfur containing polyol structure will also have a profound effect on mechanical, chemical, thermal and anticorrosive properties. Present research work reveals the preparation of polyol derived from cardanol via thiol-ene coupling. Further, the synthesized polyol was cured with various isocyanates, viz., N-75 (HDI based), Z-4470 (IPDI based) and L67 (TDI based) to yield polyurethane coatings. Moreover,

coatings were evaluated for performance properties, including mechanical, chemical, optical, anticorrosive and thermal. In addition, the structure-property relationship was established with respect to isocyanates used for curing.

2 MATERIALS

Cardanol (NC-700) was provided by Cardolite Specialty Chemicals Ltd., Mangalore, India. All analytical grade chemicals, including thioglycerol, 1,8-Diazabicycloundec-7-ene (DBU) and Irgacure 184 were purchased from SD Fine Chemicals, Mumbai, and were used as received. Desmodur N-75 (aliphatic polyisocyanate based on hexamethylene diisocyanate; % non-volatile matter [NVM]: 75, % NCO: 16.5, EW: approx. 255), Desmodur Z-4470 (cycloaliphatic polyisocyanate based on isophorone diisocyanate; % NVM: 70, % NCO: 11.9, EW: approx. 360), and Desmodur L-67 (aromatic polyisocyanate based on toluene diisocyanate; % NVM: 67, % NCO: 11.9, EW: approx. 350) were kindly supplied by Bayer MaterialScience, Mumbai, India. Commercial acrylic polyol (R-946; % NVM: 100; Hydroxyl Value: 100–105 mg of KOH/g) was received from Resins & Plastics Ltd., Mumbai, India.

3 EXPERIMENTAL

3.1 Synthesis of Cardanol-Based Polyol (Card-S-ol)

Cardanol-based polyol was synthesized and confirmed as explained in our previous study [33] and the structure of Card-S-ol is shown in Figure 1.

3.2 Coating Preparation

Mild steel panels were manually cleaned before application. Cleaning involved degreasing, hand scrubbing using emery paper (120 no.) followed by acetone
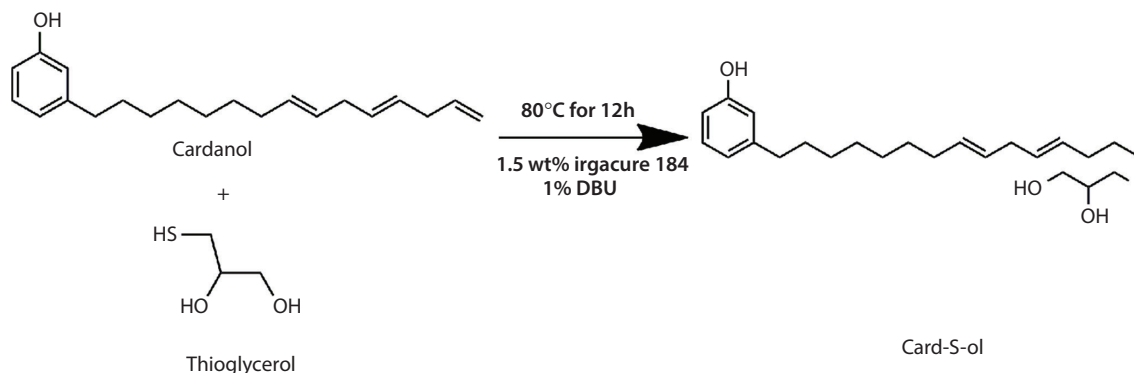

Figure 1. Structure of Card-S-ol.

cleaning. The application viscosity of all the coating solutions was maintained at 60% NVM using a mixture of xylene and butyl acetate in 70:30 wt% ratios. The coating solutions were deposited onto prepared substrate by flow method. The coated substrates were allowed to flash-off for 10 minutes at room temperature and then placed in an air circulating oven to cure at 120 °C for 15–20 minutes. The typical dry film thickness of coating was observed to be in the range of 50–60 microns. Completely cured panels were evaluated for mechanical, solvent and chemical resistance, hydrolytic stability, accelerated weathering and electrochemical properties as per ASTM standards. For a comparative study, commercial acrylic polyol was used (% NVM: 100 and Hydroxyl value: 100–105 mg of KOH/g of sample). Coatings based on Card-S-ol were represented by the letter "S" followed by isocyanate curing agent and coatings based on acrylic polyol were represented by the letter "A" followed by isocyanate curing agent. The amount of isocyanates required for curing was calculated by following Equation 1:

$$\frac{\text{Weight of isocyanate}}{\text{Equivalent weight of isocyanate}}$$
$$= \frac{\text{Weight of polyol}}{\text{Equivalent weight of polyol}} \quad (1)$$

4 CHARACTERIZATION

The gel content (GC) was determined by keeping a known weight of sample (w0) into 20 ml THF for 24 h. After 24 h, the entire mixture was filtered and the contents on the filter paper were dried in an oven at 50 °C and weighed again (w1). GC was then calculated using Equation 2:

$$\text{Gel content}\,(\%) = \frac{\text{w1} \times 100}{\text{w0}} \quad (2)$$

To measure water absorption of crosslinked samples (ASTM D570), a piece of cured film with known weight was kept in water at room temperature for 24 h. After 24 h of immersion, the sample was taken out and any drops of water left on the polymer surface were soaked with cotton. The sample was then weighed, and the weight gain was then calculated from the difference in the weights of the sample before and after soaking in water according to Equation 3:

$$\text{Water absorption}\,(\%) = \frac{(\text{Wafter} - \text{Wbefore}) \times 100}{\text{Wbefore}} \quad (3)$$

where W_{after} is the weight of the sample after dipping in water and W_{before} is the weight of the sample before dipping in water.

Coating thickness was measured as per ASTM D1186 (Test method B). Applied coatings were evaluated for adhesion properties by cross-cut adhesion with commercial cellophane tape (25-mm-wide semi-transparent tape manufactured by Permacel, New Brunswick, NJ) according to ASTM D3359. Pull-off adhesion strength of coatings was evaluated by portable adhesion tester as per ASTM D4591. Gloss of the coatings was determined according to ASTM D523. Pencil hardness and scratch hardness of the coating was measured on a hardness tester according to ASTM D3363 and IS 104. Flexibility and load distribution property of the coating were tested by conical mandrel and impact tester as per ASTM D522 and ASTM D2794 respectively. Impact resistance was measured on the impact tester with maximum height of 23.62 inches and load of 3 lbs. The abrasion resistance was measured according to ASTM D4060 using CS-17 wheels for 1000 cycles and was reported in terms of weight loss. The solvent resistance of the coatings was evaluated by double rub method according to ASTM D4752-10. The chemical resistance of the coated panels was evaluated by acid and alkali as well as water immersion method according to ASTM D1308 and ASTM D870 respectively. The degree of adhesion and visual inspection of blisters and cracks was evaluated for coated panels after immersion for 24 h. The solvent resistance was measured by a rub test using methyl ethyl ketone and xylene as per ASTM D5402. Hydrolytic stability was evaluated according to ASTM D1308; coated panel was immersed in boiling water for 4 h and evaluated for loss of adhesion and blister formation, if any.

5 INSTRUMENTATION

Glass transition temperature (T_g) and curing temperature (T_{ct}) measurement was performed by differential scanning calorimetry (DSC) on DSC Q100 equipment (TA Instruments, USA). For the evaluation of T_g, the samples were evaluated in two heating cycles of 40 to 100 °C and –20 to 100 °C at a heating rate of 10 °C/min under nitrogen atmosphere. For the evaluation of T_{ct}, all samples were heated from –20 to 150 °C at a heating rate of 10 °C/min. The thermogravimetric analysis (TGA) of coating samples was performed on a TGA Q-500 (TA Instruments, USA) Compatibilization, elastomer, PPO/PA11 blends, toughening under nitrogen atmosphere for the temperature range of 40–600 °C at a heating rate of 10 °C/min. The wide angle X-ray diffraction (XRD) patterns were evaluated using a MiniFlex X-ray diffractometer (Rigaku Europe, Germany). The 2θ diffraction was scanned from

J. Renew. Mater. Vol. 6, No. 5, August 2018

© 2018 Tech Science Press 519

2° to 80° at intervals of 0.05°. The percentage crystallinity was calculated from the integral of crystalline area and integral of total area. The anticorrosive performance of the coated panels was evaluated by electrochemical impedance spectroscopy (EIS) and Tafel analysis. For this, a VersaSTAT-3 instrument (AMETEK, Princeton Applied Research, Oak Ridge, TN) was used and all electrochemical measurements were obtained at room temperature (30 °C) in 3.5% NaCl solution. Test system consisted of three electrode cells, in which a calomel electrode, a platinum electrode and a coated panel were used as reference, counter and working electrode respectively. The area of the coated panels exposed to the NaCl solution was 7 cm² in all the cases and corrosion rate was calculated using the formula [34]. Salt spray testing was conducted in a salt spray chamber containing 5% NaCl solution. All the experiments were conducted in duplicate to ensure the repeatability and consistency of the results.

6 RESULTS AND DISCUSSION

Confirmation of Card-S-ol was done by determining hydroxyl and iodine values as well as characterization by FTIR, ¹H-NMR spectroscopies and gel permeation chromatography.

6.1 Coating Properties

Coating properties are majorly governed by functionality of polymer, chemical structure of polymer backbone, nature and chemical structure of curing agent, its functionality, etc. [35]. Card-S-ol is trifunctional in nature and contains one aromatic ring and one C15 aliphatic chain. To effect crosslinking, curing agents varying in chemical structures, such as N-75, Z-4470

and L-67, were selected in order to study the effect of these curing agents on the final performance properties of PU coatings. In this case, N-75 is aliphatic polyisocyanate, Z-4470 is cycloaliphatic and L-67 is aromatic in nature. Such varying nature of curing agents causes changes in mechanical, chemical, thermal and anticorrosive properties.

6.1.1 Mechanical Properties

All the coatings were applied onto mild steel panels with an average DFT of 40–55 microns and allowed to cure at 120 °C for 15–20 minutes. Completely cured coatings were evaluated for mechanical, chemical, optical, anticorrosive and thermal properties. All the coatings showed excellent adhesion to the metal substrate as indicated by the 5B rating. However, acrylic-PU coatings exhibited slightly higher values of pull-off adhesion as compared to that of Card-S-ol–PU coatings. Gel content was observed to be above 90%, suggesting that excellent crosslinking was achieved in the case of all coatings. Gloss of cardanol-based coatings was observed to be slightly higher than that of corresponding acrylic coatings. Moreover, coatings cured with L-67 showed the highest gloss values (as shown in Table 1). Inherent aromatic ring present in cardanol and L-67 resulted in an orderly structure, which is responsible for high reflectivity and hence gloss values. Similarly, pencil hardness and scratch hardness of coatings cured with L-67 were observed to be the highest amongst all. Both Card-S-ol and acrylic-PU coatings exhibited excellent hardness values. In addition, Card-S-ol coatings showed better scratch hardness as compared to that of their corresponding acrylic counterpart. Load distribution property of cardanol-based PU coatings was observed to be excellent; however,

Table 1. Mechanical and physicochemical properties of coatings.

Characterization	S-N75	S-Z4470	S-L67	A-N75	A-Z4470	A-L67
Gloss@60°	90–95	105–110	120–125	75–80	95–100	110–120
Gel content (%)	93.83	94.58	95.18	90.62	91.44	90.56
Adhesion	5B	5B	5B	5B	5B	5B
Pull-off adhesion (MPa)	1.10	1.63	1.53	2.22	2.54	2.68
Pencil hardness	6H	6H	6H	5H	6H	6H
Scratch hardness (kg)	2.5	2.7	2.8	1.8	1.9	2.1
Impact resistance (lbs.inch)						
Intrusion	70.86	70.86	70.86	70.86	64.96	47.24
Extrusion	70.86	70.86	70.86	70.86	35.43	23.62
Flexibility (mm)	0	0	0	0	4	9
Abrasion resistance (weight loss in mg after 1000 cycles)	6.7	4.1	1.8	7.8	5.3	2.3
Water absorption (%)	1.8	1.6	1.5	2.0	1.8	1.4

acrylic coatings cured with Z-4470 and L-67 showed poor extrusion impact. Presence of cycloaliphatic and aromatic structure in Z-4470 and L-67 respectively resulted in brittle coating films and therefore suffered poor impact resistance. The aliphatic nature of HDI-based N-75 could distribute the load evenly over the entire coating surface, thereby showing excellent impact resistance. A similar trend was observed in the case of flexibility, where coatings cured with N-75 showed excellent flexibility as compared to those coatings cured with Z-4470 and L-67 crosslinkers [36]. In addition, the impact and flexibility of cardanol-based PU was observed to be higher as compared to that of acrylic-PU coatings. The presence of C15 aliphatic chain in cardanol could be the reason for the excellent load distribution property of Card-S-ol–PU coatings. Further, abrasion resistance of cardanol-based PU was slightly better than that of acrylic PU. The hard and compact structure of L-67 cured coatings was responsible for the exhibition of superior abrasion resistance amongst all. Water absorption values were observed to be almost similar in the case of both systems and ranged from 1.4–2%.

6.1.2 X-Ray Diffraction (XRD) Analysis

To evaluate crystalline and amorphous regions in the coatings, XRD diffractograms of all PU coatings were performed and are shown in Figure 2. As expected, % crystallinity of L67 cured coatings was the highest amongst the series, followed by coatings cured with Z4470 and the least for coatings cured with N75 (as shown in Table 2). Irrespective of isocyanate curing agents, acrylic PU coatings exhibited lower values of % crystallinity than that of cardanol-based PUs. The trifunctional nature of Card-S-ol and presence of aromatic ring might be responsible for higher values of % crystallinity of coatings.

6.1.3 Chemical Properties

Chemical resistance of coatings was evaluated by immersion of coated panels in 5% HCl and 5% NaOH

Table 2. % Crystallinity of films.

Coatings	% Crystallinity
S-N75	4.82
S-Z4470	8.43
S-L67	10.37
A-N75	3.98
A-Z4470	6.37
A-L67	9.91

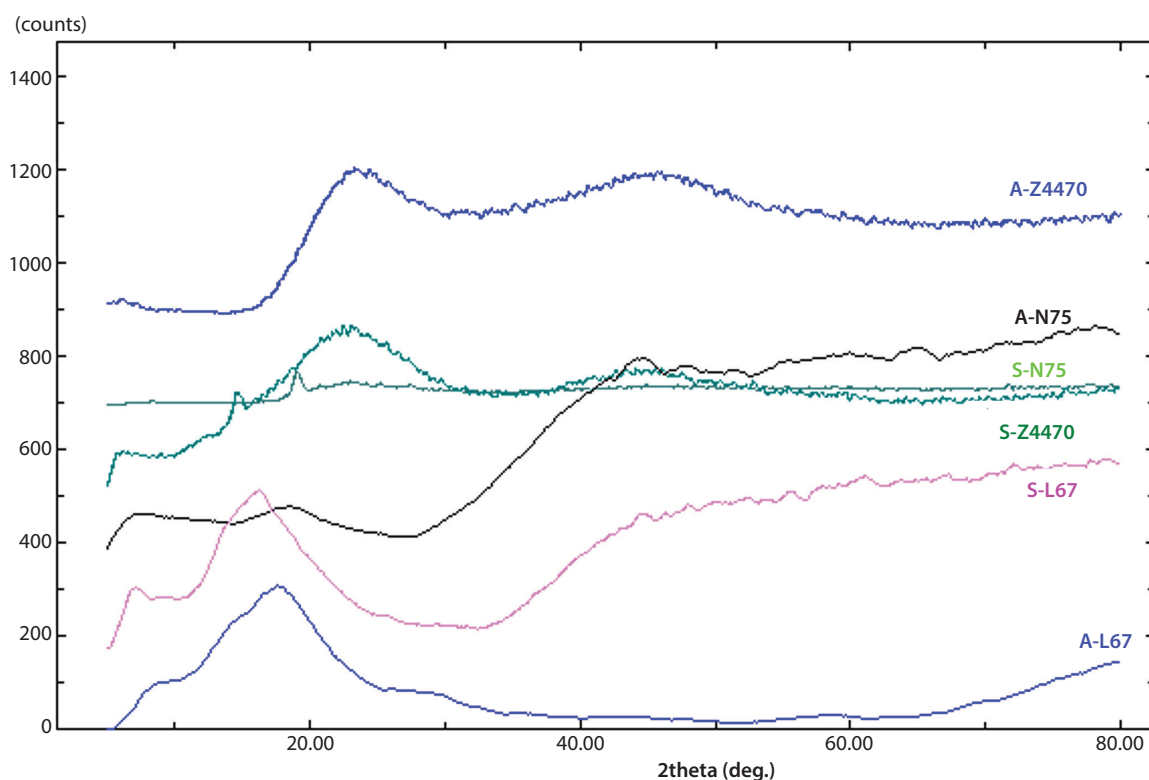**Figure 2.** XRD of polyurethane coatings.

J. Renew. Mater. Vol. 6, No. 5, August 2018

© 2018 Tech Science Press 521

solution for 24 h and expressed in Table 3. It was observed that all the coatings exhibited excellent resistance to acid and alkali as no film defects, such as loss of gloss, etching of film, softening of film, etc., were observed. Hydrolytic stability evaluated by dipping the coated panels in boiling water for 4 h suggested that except for A-N75, all the coatings showed excellent hydrolytic stability as no film defects, such as delamination, blisters or loss of gloss, were observed on the panels. The presence of cycloaliphatic and aromatic structure in Z4470 and L67 restricted the permeation of water through the coating, thereby exhibiting good hydrolytic stability; whereas aliphatic N75 allowed easy penetration of water through the coating, showing poor hydrolytic stability. Solvent resistance was evaluated by solvent rub method using methyl ethyl ketone (MEK) and xylene solvents. All the coatings

showed excellent resistance towards xylene, however, exhibited poor resistance to MEK. Coatings based on Card-S-ol as well as acrylic polyol showed poor MEK resistance irrespective of the hardener used for curing. This could be due to the polar urethane linkages present in the coatings that might get solubilized in MEK.

6.1.4 Thermal Properties

6.1.4.1 Glass Transition Temperature

All the coatings were evaluated using DSC thermograms in order to determine the glass transition temperature of PU films and the results are shown in Figure 3. Glass transition temperature of the coatings is mainly dependent on the crosslink density and mobility of polymer chains. It was observed that glass transition temperatures of Card-S-ol–PU coatings were

Table 3. Chemical resistance of coatings.

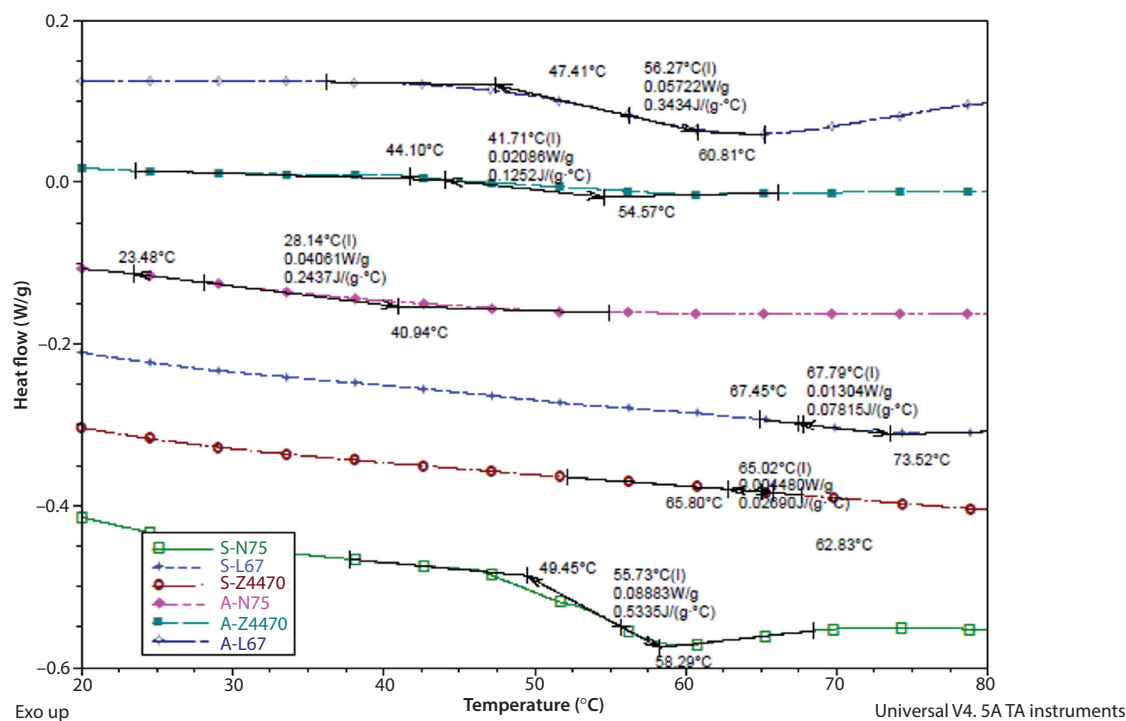| Coatings	Acid resistance	Alkali resistance	Hydrolytic stability	Solvent resistance	
				MEK	Xylene
S-N75	Pass	Pass	No defects	< 150	> 200
S-Z4470	Pass	Pass	No defects	< 170	> 200
S-L67	Pass	Pass	No defects	< 200	> 200
A-N75	Pass	Pass	Softening	< 150	> 200
A-Z4470	Pass	Pass	No defects	< 200	> 200
A-L67	Pass	Pass	No defects	> 200	> 200

Figure 3. Glass transition temperature as evaluated by DSC.

higher than their acrylic counterpart. It can be attributed to the aromatic ring present in the cardanol and additional phenolic OH present in cardanol that take part in curing reaction, resulting in a compact three-dimensional crosslinked network [37]. As can be seen from Table 4, the highest T_g was observed in the case of coatings cured with L67, followed by those cured with Z4470 and the least for N75 [35]. The nature of isocyanates greatly affects the crosslink density of the coatings. L67 possesses aromatic rings that imparted hard and compact structure to the coatings resulting in higher values of T_g, followed by Z4470 which contains cycloaliphatic structure; while the presence of aliphatic chain in N75 was responsible for reducing the T_g of coatings. Thus, in the case of Card-S-ol–PU

Table 4. Curing temperature and glass transition temperature of the coatings.

Coatings	T_g (°C)	Tcuring (°C)
S-N75	55.7	91.8
S-Z4470	65.0	72.9
S-L67	67.7	66.7
A-N75	28.1	81.9
A-Z4470	41.7	63.6
A-L67	56.2	59.2

coatings, T_g values ranged from 55–67 °C, while in the case of acrylic-PU coating it ranged from 28–56 °C.

6.1.4.2 Curing Temperature

Curing temperatures of all the compositions were investigated using DSC analysis and are shown in Figure 4. All the formulations were mixed in stoichiometric proportion and heated from –15 °C to 120 °C at a heating rate of 10 °C/min. For all the coatings, curing temperature was observed to be below 100 °C, as shown in Table 4. Further, it was observed that acrylic-PU coatings exhibited lower curing temperature as compared to their Card-S-ol–PU counterpart. As we know, phenolic OH requires a higher temperature to react with isocyanates, which could be the possible reason for higher values of curing temperatures for Card-S-ol–PU coatings. Moreover, coatings cured with L-67 showed the lowest curing temperature, followed by those cured with Z-4470 and the least for N-75.

6.1.4.3 Thermogravimetric Analysis

Thermogravimetric analysis was carried out to study the degradation behavior of PU coatings and is shown in Figure 5. All the coatings exhibited one-step degradation behavior irrespective of curing agent used. As can be seen from Table 5, initial decomposition temperature of coatings based on cardanol was higher as
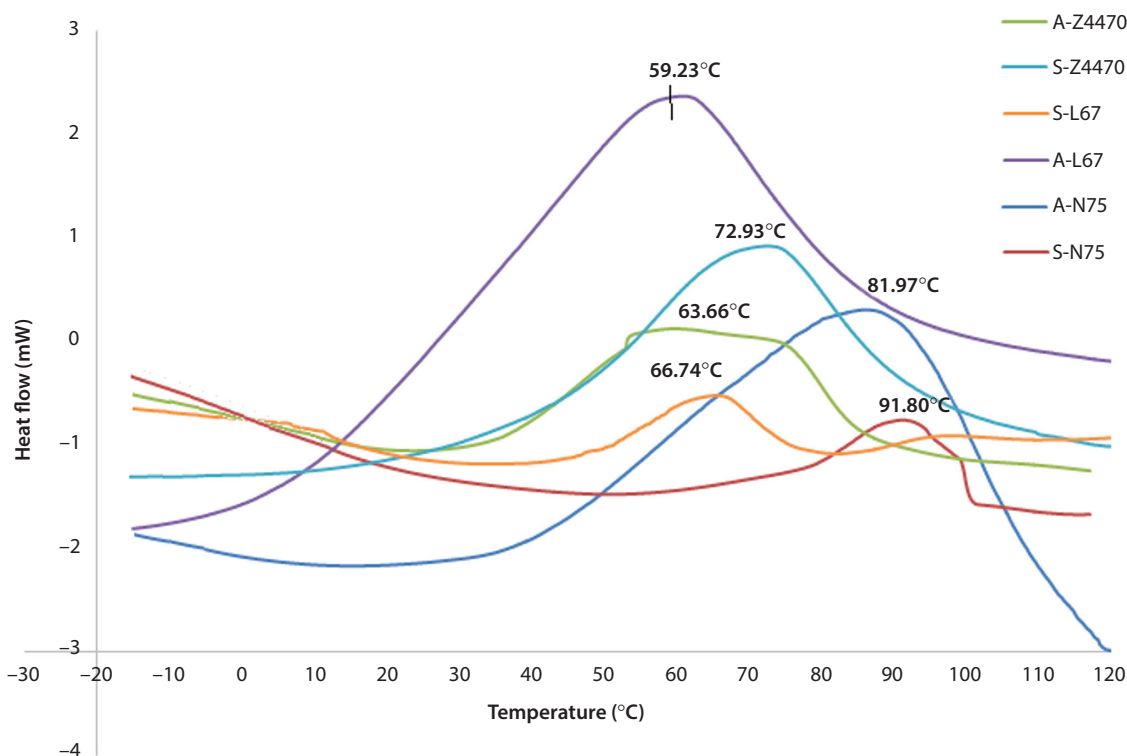

Figure 4. Curing temperatures of coatings at heating rate 10 °C/min.
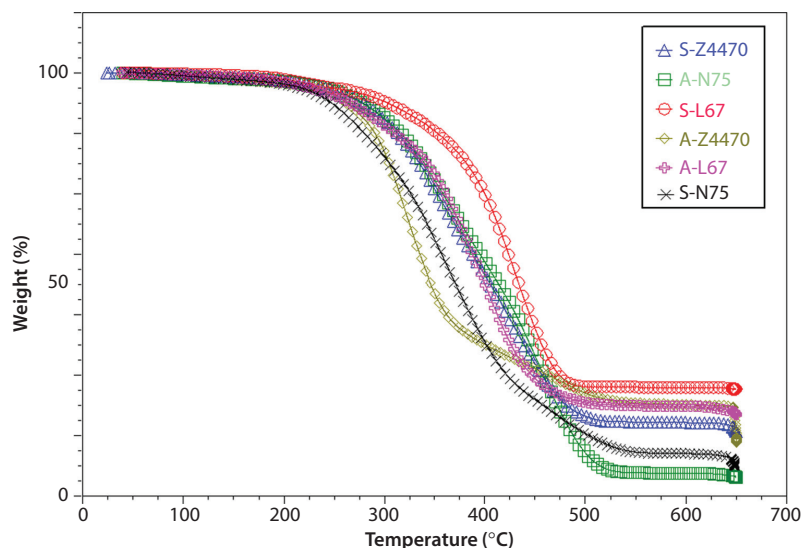
J. Renew. Mater. Vol. 6, No. 5, August 2018

© 2018 Tech Science Press 523

Figure 5. TGA curves of coatings.

Table 5. TGA values of coatings.

Coatings	$T_{10\%}$ (°C)	Tonset (°C)	Toffset (°C)	Char yield (%)
S-N75	269	264	446	9.71
S-Z4470	273	300	468	16.85
S-L67	289	369	478	25.31
A-N75	233	339	435	5.2
A-Z4470	252	283	370	19.57
A-L67	254	324	443	21.42

compared to those obtained with acrylic system. This could be attributed to the presence of aromatic ring in the cardanol structure. Initial degradation temperature of Card-S-ol–PU system was observed to be in the range of 250–370 °C. Initially, degradation of urethane linkages took place at around 200–300 °C and isocyanates, amines and alcohols were released [38]. Above 300 °C, decomposition of C15 aliphatic chain of cardanol occurred. It was also observed that coatings cured with L67 exhibited excellent thermal stability, followed by coatings cured with Z4470 and the least for coatings cured with N75. The inherent structure of isocyanates was responsible for such a trend in the thermal stability. The aromatic and cycloaliphatic nature of L-67 and Z-4470 provided more thermal stability to the coatings than that of the coatings cured with aliphatic N-75. The % char yield of Card-S-ol–PU system was also comparatively higher than its acrylic-PU counterpart.

6.1.5 Anticorrosive Properties

Anticorrosive properties of coatings were evaluated using electrochemical impedance spectroscopy (EIS),

Tafel analysis and salt spray testing. Salt spray testing was conducted wherein coated panels were exposed to 3.5 wt% aqueous solution of NaCl at 35 °C for 500 h. Salt spray images of coated panels before and after 500 h of exposure are shown in Figures 6 and 7 respectively. It was observed that Card-S-ol–PU coatings exhibited slightly better anticorrosion resistance than that of corresponding acrylic-PU coatings. After 500 h of exposure, acrylic-PU coatings showed serious blister formation, whereas no such film defect was observed on the Card-S-ol coatings. Further, panels were rated for creepage from scribe and % area failed as per ASTM D1654, and the values are summarized in Table 6. In addition, coatings cured with L-67 showed the highest corrosion resistance amongst the series.

Resistance offered by coating to alternating current was evaluated by EIS measurement. Corrosion resistance of coatings depends on the hard and rigid moieties present in the polymer backbone, functionality and chemical structure of crosslinker. As can be seen from Figure 8, it can be observed that cardanol-based coatings showed better impedance values compared to their acrylic counterpart. Excellent impedance values
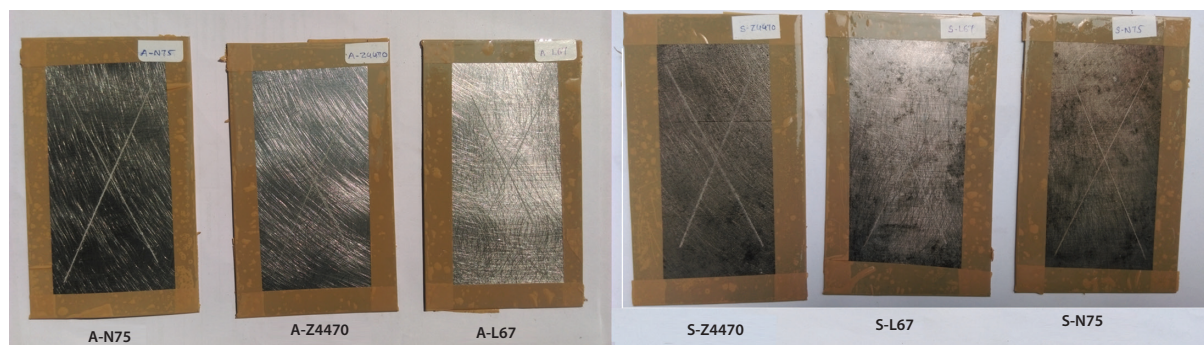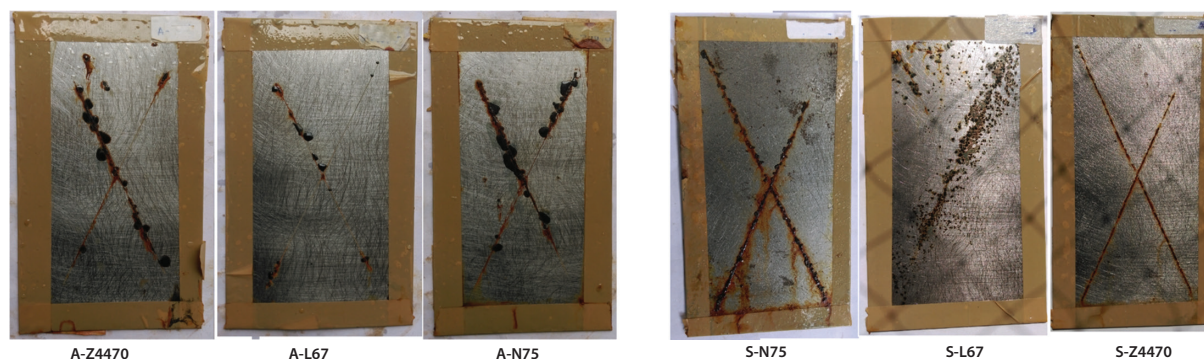
Figure 6. Coated panels before exposure.

Figure 7. Coated panels after exposure for 500 h.

Table 6. Ratings for creepage values and % area failed of coatings.

Coatings	Average creepage from scribe	% area failed
S-N75	6	7
S-Z4470	7	7
S-L67	10	10
A-N75	5	8
A-Z4470	6	8
A-L67	8	9

Note: 10: Excellent, 0: Worst

of cardanol-based coatings can be related to a number of factors such as aromatic ring of cardanol, corrosion inhibition action of sulphur atom [39–40], hydrophobicity of the coating, etc.

All these factors increase the barrier properties at the surface of coating, thereby avoiding the electrochemical reactions at the surface and providing excellent corrosion resistance. Here also, coatings cured with L-67 exhibited excellent impedance values followed by those cured with Z-4470, and N-75 cured coatings being the least amongst the series. Similar results were obtained in Tafel analysis (shown in Fig. 9) where cardanol-based PU exhibited higher potential

values, lower current values and lower corrosion rates (as shown in Table 7) when compared to acrylic-PU coatings. In this case, N75 is aliphatic polyisocyanate based on HDI whereas Z4470 is cycloaliphatic polyisocyanate based on IPDI and L67 is aromatic polyisocyanate based on TDI; amongst which, reactivity of TDI is much higher and aromatic ring in its structure develops excellent crosslinked structure and therefore superior corrosion resistance. Similarly, the cycloaliphatic nature of Z4470 also imparted somewhat similar hard and rigid structure to the coating films. Whereas, the aliphatic nature of N-75 allowed easy permeation of corroding species through the coatings and exhibited poor corrosion resistance. Moreover, S-L67 showed the lowest corrosion rate in the series followed by S-Z4470 and then S-N75.

7 CONCLUSION

Cardanol-based polyurethane coatings were successfully prepared via thiol-ene addition. Card-S-ol was cured with various polyisocyanates, such as N-75, Z-4470 and L-67, and characterized for performance properties. It was observed that cardanol-based PU coatings exhibited excellent mechanical, chemical, thermal and anticorrosive properties as compared to
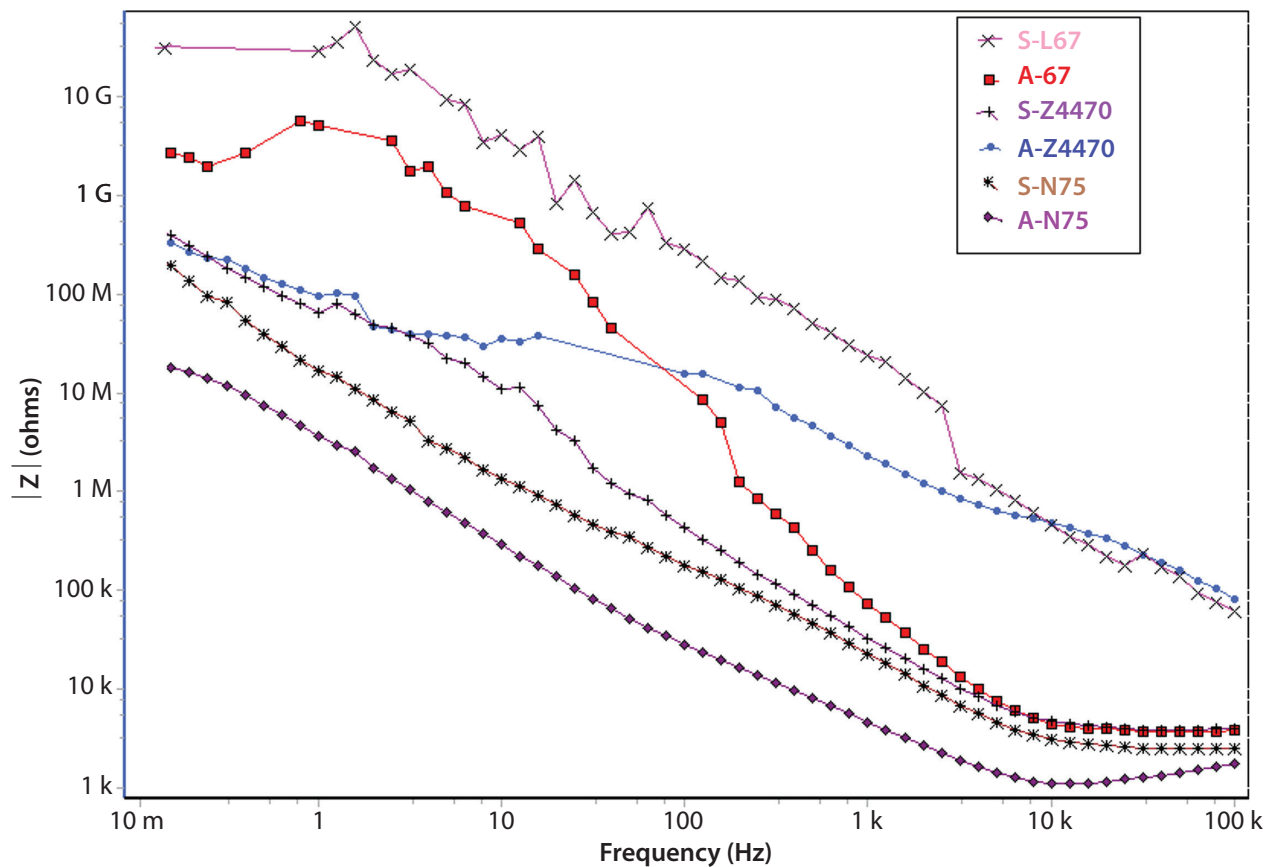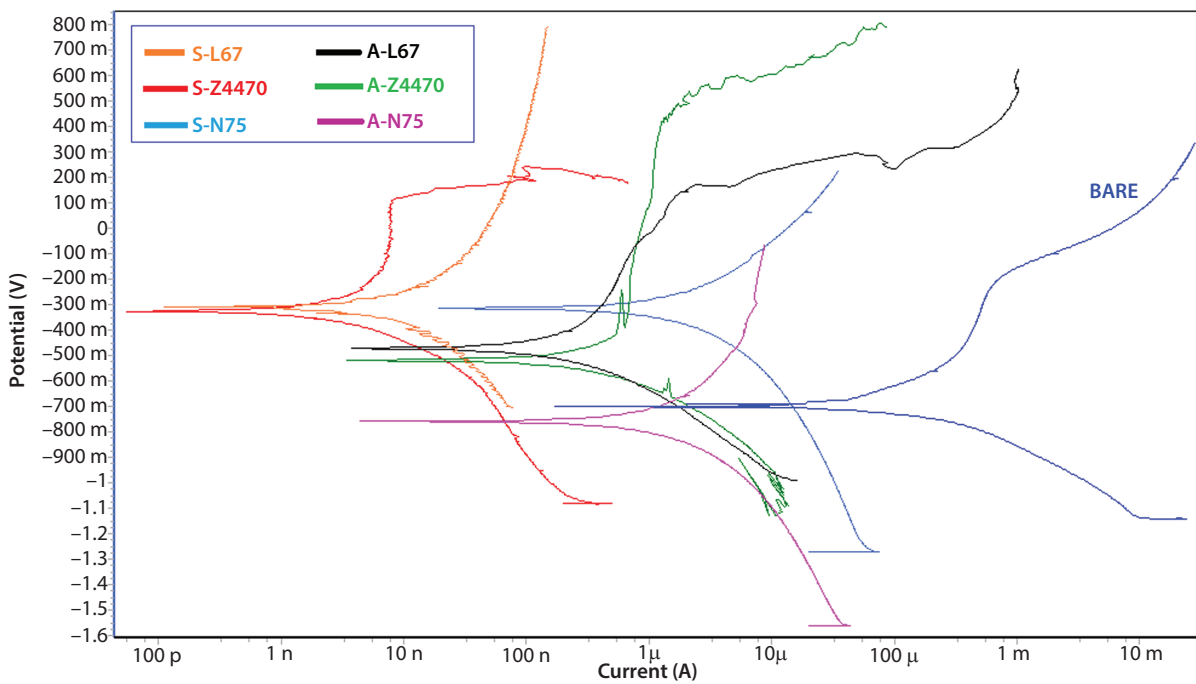
Figure 8. Bode plot of coatings.

Figure 9. Tafel plots of coatings.

526   *J. Renew. Mater.* Vol. 6, No. 5, August 2018

© 2018 Tech Science Press

Table 7. Tafel plot values for coatings.

Coatings	Potential (mV)	Current (A)	Corrosion rate (mmpy)
Bare	–719.21	2.33E-04	3.88E-01
S-N75	–361.57	8.40E-07	1.39E-03
S-Z4470	–336.13	3.5E-09	5.81E-06
S-L67	–309.83	2.01E-09	3.32E-06
A-N75	–760.12	3.44E-07	5.72E-04
A-Z4470	–502.15	2.94E-07	4.88E-04
A-L67	–476.23	2.08E-08	3.45E-04

that of commercial acrylic-PU coatings. The superior performance properties of cardanol-based PU coatings were attributed to the presence of aromatic ring, sulphur atom in the structure, hydrophobic C15 long aliphatic chain in cardanol as well as urethane linkages present in the coatings.

ACKNOWLEDGMENT

REFERENCES

1. R. Quirino, T. Garrison, and M. Kessler, Matrices from vegetable oils, cashew nut shell liquid, and other relevant systems for biocomposite applications. *Green Chem.* **16**, 1700–1715 (2014).
2. G. Wu, X. He, H. Zhang, and Y. Yan, Synthesis and characterization of biobased polyurethane/SiO2 nanocomposites from natural sebiferum oil. *RSC Adv.* **5**, 27097–27106 (2015).
3. T. Nelson, B. Masaki, Z. Morseth, and D. Webster, Highly functional bio-based polyols and their use in melamine-formaldehyde coatings. *J. Coat. Tech. Res.* **10**, 757–767 (2013).
4. C. Zhang, S. Madbouly, and M. Kessler, Biobased polyurethanes prepared from different vegetable oils. *ACS Appl. Mater. Interfaces* **7**, 1226–1233 (2015).
5. C. Zhang and M. Kessler, Bio-based Polyurethane Foam Made from Compatible Blends of Vegetable-Oil-based Polyol and Petroleum-based Polyol. *ACS Sustain. Chem. Eng.* **3**, 743–749 (2014).
6. O. Turunc and M. Meier, Fatty acid derived monomers and related polymers via thiol-ene (Click) additions. *Macromol. Rapid Commun.* **31**, 1822–1826 (2010).
7. K. Suresh, Rigid polyurethane foams from cardanol: Synthesis, structural characterization, and evaluation of polyol and foam properties. *ACS Sustain. Chem. Eng.* **1**, 232–242 (2013).
8. D. Balgude and A. Sabnis, An environment friendly alternative for the modern coating industry. *J. Coat. Tech. Res.* **11**, 169–183 (2014).
9. M. Lubi and E. Thachil, Cashew nut shell liquid (CNSL) — A versatile monomer for polymer synthesis. *Des. Monomers Polym.* **3**, 123–153 (2000).
10. D. Balgude, K. Konge, and A. Sabnis, Synthesis and characterization of sol–gel derived CNSL based hybrid anti-corrosive coatings. *J. Sol-Gel Sci. Technol.* **69**, 155–165 (2014).
11. M. Kathalewar, A. Sabnis, and D. D'Mello, Isocyanate free polyurethanes from new CNSL based bis-cyclic carbonate and its application in coatings. *Eur. Polym. J.* **57**, 99–108 (2014).
12. I. Omrani, A. Farhadian, N. Babanejad, H. Shendi, A. Ahmadi, and M. Nabid, Synthesis of novel high primary hydroxyl functionality polyol from sunflower oil using thiol-yne reaction and their application in polyurethane coating. *Eur. Polym. J.* **82**, 220–231 (2016).
13. A. Pauly and F. Lena, Incorporating amino acid sequences into the backbone chain of polymers through thiol-ene chemistry. *Polymer* **72**, 378–381 (2015).
14. C. Hoyle and C. Bowman, Thiol-ene click chemistry. *Angew. Chem. Int. Ed.* **49**, 1540–1573 (2010).
15. M. Podgórski, E. Becka, M. Claudino, A. Flores, P. Shah, J. Stansbury, and C. Bowman, Ester-free thiol-ene dental restoratives. Part A: Resin development. *Dent. Mater.* **11**, 1255–1262 (2015).
16. D. Nair, M. Podgorski, S. Chatani, T. Gong, W. Xi, C. Fenoli, and C. Bowman, The thiol-Michael addition click reaction: A powerful and widely used tool in materials chemistry. *Chem. Mater.* **26**, 724–744 (2014).
17. A. Lowe, Thiol-yne 'click-coupling chemistry and recent applications in polymer and materials synthesis and modification. *Polymer* **55**, 5517–5549 (2014).
18. C. Hoyle, T. Lee, and T. Roper, Thiol-enes: Chemistry of the past with promise of the future. *J. Polym. Sci. Part A: Polym. Chem.* **42**, 5301–5338 (2004).
19. C. Hoyle, A. Lowe, and C. Bowman, Thio-click chemistry: A multifaced toolbox for small molecule and polymer synthesis. *Chem. Soc. Rev.* **39**, 1355–1387 (2010).
20. D. Guzman, X. Ramis, X. Francos, and A. Serra, Preparation of click thiol-ene/thiol-epoxy thermosets by controlled photo/thermal dual curing sequence. *RSC Adv.* **5**, 101623–101633 (2015).
21. Y. Duo, Y. Ping, D. Fang, S. Jin, J. Wa, G. Mou, Y. Yu, L. Yang, and L. Chin, Chemically bonded polyacrylamide via thiol-ene click chemistry as separation materials for hydrophilic interaction liquid chromatography. *J. Anal. Chem.* **43**, 1439–1444 (2015).
22. T. Yoshimura, T. Shimasaki, N. Teramoto, and M. Shibata, Bio-based polymer networks by thiol-ene photopolymerizations of allyl-etherified eugenol derivatives. *Eur. Polym. J.* **67**, 397–408 (2015).

23. M. Stemmelen, F. Pessel, V. Lapinte, S. Caillol, J. Habas, and J. Robin, A fully biobased epoxy resin from vegetable oils: From the synthesis of the precursors by thiol-ene reaction to the study of the final material. *J. Poly. Sci. Part A: Poly. Chem.* **49**, 2434–2444 (2011).

24. T. Hayashi, A. Kazlauciunas, and P. Thornton, Dye conjugation to linseed oil by highly-effective thiol-ene coupling and subsequent esterification reactions. *Dyes Pigm.* **123**, 304–316 (2015).

25. O. Turunc and M. Meier, The thiol-ene (click) reaction for the synthesis of plant oil derived polymers. *Eur. J. Lipid Sci. Technol.* **41**, 41–54 (2013).

26. P. Alagi, Y. Choi, and S. Hong, Preparation of vegetable oil based polyols with controlled hydroxyl functionalities for thermoplastic polyurethanes. *Eur. Polym. J.* **78**, 46–60 (2016).

27. Z. Chen, B. Chisholm, R. Patani, J. Wu, S. Fernando, K. Jogodzinski, and D. Webster, Soy-based UV curable thiol-ene coatings. *J. Coat. Tech. Res.* **7**, 603–613 (2010).

28. D. Echeverri, V. Cadiz, J. Ronda, and L. Rios, Synthesis of elastomeric networks from maleated soybean oil glycerides by thiol-ene coupling. *Eur. Polym. J.* **48**, 2040–2049 (2012).

29. M. Black and J. Rawlins, Thiol-ene UV curable coatings using vegetable macromonomers. *Eur. Polym. J.* **45**, 1433–1441 (2009).

30. A. Luo, X. Jiang, H. Lin, and J. Yin, Thiol-ene photocured hybrid materials based on POSS and renewable vegetable oil. *J. Mater. Chem.* **21**, 12753–12760 (2011).

31. C. Fu, J. Liu, H. Xia, and L. Shen, Effect of structure on the properties of polyurethanes based on aromatic cardanol-based polyols prepared by thiol-ene coupling. *Prog. Org. Coat.* **83**, 19–25 (2015).

32. H. Kolb, M. Finn, and K. Sharpless, Click chemistry: Diverse chemical function from a few good reactions. *Angew. Chem. Int. Ed. Engl.* **40**, 2004–2021 (2001).

33. K. Wazarkar and A. Sabnis, Development of cardanol based polyol via click chemistry and crosslinking with melamine formaldehyde resin for coating applications. *J. Renew. Mater.* **5**, 3–4 (2017).

34. K. Wazarkar, M. Kathalewar, and A. Sabnis, High performance polyurea coatings based on cardanol. *Prog. Org. Coat.* **106**, 96–110 (2017).

35. K. Griesbaum, Problems and possibilities of the free radical addition of thiols to unsaturated compounds. *Angew. Chem. Int. Ed.* **9**, 273–287 (1970).

36. D. Balgude, A. Sabnis, and S. Ghosh, Synthesis and characterization of cardanol based aqueous 2K polyurethane coatings. *Eur. Polym. J.* **85**, 620–634 (2016).

37. R. Liu, X. Zhang, J. Zhu, X. Liu, Z. Wang, and J. Yan, UV-curable coatings from multi-armed cardanol based acrylate oligomers. *ACS Sustain. Chem. Eng.* **3**, 1313–1320 (2015).

38. M. Kathalewar, A. Sabnis, and D. D'Melo, Polyurethane coatings prepared from CNSL based polyols: Synthesis, characterization and properties. *Prog. Org. Coat.* **77**, 616–626 (2014).

39. M. Takashima, Electronic parts cleaning solution, US Patent 6472357 B2, assigned to Sumitomo Chemical Company, Limited (2002).

40. M. Takashima and K. Sawara, Metal corrosion inhibitor and cleaning liquid, US Patent 6200947 B1, assigned to Sumitomo Chemical Company, Limited (2001).

Supplementary Document Available Online

http://www.scrivenerpublishing.com/journalsuppl/jrm/JRM-2017-0098/jrm_JRM-2017-0098_supp1.tif